Research Article Open Access

Jan Čech*, Jana Hanusová, Pavel Sťahel, Mirko Černák

# Diffuse Coplanar Surface Barrier Discharge in Artificial Air: Statistical Behaviour of Microdischarges

**Abstract:** Diffuse Coplanar Surface Barrier Discharge (DCSBD) is a novel type of atmospheric-pressure plasma source developed for high-speed large-area surface plasma treatments. The statistical behavior of microdischarges of DCSBD generated in artificial air atmosphere was studied using time-correlated optical and electrical measurements. Changes in behavior of microdischarges are shown for various electrode gap widths and input voltage amplitudes. They are discussed in the light of correlation of the number of microdischarges and the number of unique microdischarges' paths per discharge event.

The 'memory effect' was observed in the behavior of microdischarges and it manifests itself in a significant number of microdischarges reusing the path of microdischarges from previous half-period. Surprisingly this phenomenon was observed even for microdischarges of the same half-period of the discharge, where mechanisms other than charge deposition have to be involved. The phenomenon of discharge paths reuse is most pronounced for wide electrode gap width and/or increased input voltage amplitude.

**Keywords:** Microdischarge, Dielectric Barrier Discharge, Statistics, Memory Effect, Air

DOI: 10.1515/chem-2015-0062
received January 22, 2014; accepted May 8, 2014.

***Corresponding author: Jan Čech:** Masaryk University, R&D center for low-cost plasma and nanotechnology surface modifications, Kotlarska 2, 611 37 Brno, Czech Republic,
E-mail: cech@physics.muni.cz
**Jana Hanusová, Pavel Sťahel, Mirko Černák**: Masaryk University, R&D center for low-cost plasma and nanotechnology surface modifications, Kotlarska 2, 611 37 Brno, Czech Republic

## 1 Introduction

The importance of dielectric barrier discharges (DBDs) as the sources of non-equilibrium plasmas for material processing has been continually increasing in past decades [1]. It follows from the current trends in industrial applications where we can see an effort to replace low-pressure plasma processing by the atmospheric-pressure systems [2,3].

Two major demands could be identified behind the increase of industrial usage of atmospheric plasma technologies: the increasing demands on the surface properties of low-added-value materials (e.g. improved wettability or printability [4]), together with the pressure put on the industry to avoid usage of harmful chemical compounds in industrial applications [5]. At least two conditions have to be fulfilled to satisfy these demands. Firstly, the atmospheric plasma processing should be uniform in the meaning of surface properties of processed materials [6–8]. Secondly, the atmospheric pressure plasma processing should be time and cost efficient [9–13].

Dielectric barrier discharges have become promising candidates to fulfil aforementioned requirements [7,14–16]. The DBD in volume configuration has been adopted for atmospheric-pressure plasma processing at first for its simple design [3,17,18]. The main drawback of the volume DBD lies in the limited thickness of processed material, as follows from its design. Another disadvantage of volume DBD lies in low energetic and time efficiency of material processing, which follows from the limited contact surface of the generated plasma with respect to the overall generated volume of plasma. Volume DBD generates plasma that is non-homogeneous in most cases. The so-called Diffuse Coplanar Surface Barrier Discharge (DCSBD) was developed to address drawbacks of the volume DBD design [19–21]. The plasma of DCSBD discharge is generated in a sub-millimeter thin layer above the dielectric plate. With gradual increase of power

input the DCSBD gets visually more and more diffuse and homogeneous, though it is still composed of a high number of individual microdischarges. The microdischarges with their properties and interactions influence in general the plasma parameters of DBD [22–25], and the DCSBD as well. It is therefore of great importance to study the parameters of individual microdischarges [26,27] as well as their collective behavior [28–30] to improve the understanding of plasma processes in DCSBD, which can be used for material treatment in industrial applications [31–35].

From the economic and practical point of view air is the most natural choice as a process gas to be used at atmospheric pressure for the plasma processing of materials. The use of air as the carrier or process gas brings both advantages and disadvantages. The main advantage of choosing air as the process gas is that it is naturally present at the industrial production lines. The air can be easily processed to the desired level of humidity and/or amount of environmental pollutants on-site and it is also completely harmless to humans and the environment as a whole. The main disadvantage of volume DBD is the fact that it generates strongly inhomogeneous (filamentary) plasma under such conditions. For the generation of homogeneous volume DBDs at atmospheric pressure the use of noble gasses or pure nitrogen is necessary – as in the case of e.g. APGD or APTD [36–39]. Contrary to the previously mentioned DBD configurations the DCSBD is capable of generating a macroscopically uniform plasma layer with high power density and energetic efficiency when operated in air [40,41]. That enables a fast and homogeneous in-line plasma treatment of materials at high-speeds e.g. 450 m $min^{-1}$ in the case of nonwoven textile [21]. Moreover, the DCSBD discharge design does not limit dimensions of the treated material, as the discharge design is of a surface type. The discharge cell can be pressed against the treated surface and the treated material does not need to be driven 'through' the discharge cell.

In the presented paper the DCSBD operated in artificial air was studied. The behavior of DCSBD microdischarges generated at the regime above ignition voltage at narrow and wide electrode distances was studied. For the presented experiments time correlated fast iCCD imaging and electrical measurement of the discharge were used. To our best knowledge the statistical parameters of microdischarges of DBD in coplanar configuration generated in air have not been described so far. We believe therefore that it can be used in further development of DCSBD as well as other types of DBD.

## 2 Experimental Setup

An industrial DCSBD electrode consists of approx. 20 pairs of coplanar strip electrodes forming a rather complex electric field distribution. Multi-pair electrode setup also induces complex interactions of microdischarges burning between adjacent electrode pairs that are not satisfactorily explained until now. The number of DCSBD microdischarges generated during one discharge period is very high (in the order of tens to hundreds of single microdischarges) and generated microdischarges are distributed above a large area of approx. 20 x 8 $cm^2$. This makes the accurate measurements of microdischarges' parameters very difficult taking into account the typical dimensions of a single microdischarge to be of the order of 1 mm of length and 100 μm of diameter in the time scale of several tens of nanoseconds. In order to better understand the key discharge properties of aforementioned DCSBD discharge, the simplified DCSBD electrode system was used in the presented study. This simplified DCSBD electrode setup consists of only one electrode pair. This setup decreases the complexity of electric field distribution on the one hand. On the other hand it also limits the interactions of microdischarges to the interactions of only adjacent and/or in sequence microdischarges generated in between the same electrode pair. This enables us to study the discharge parameters of the simplified DCSBD system, while keeping the key properties of standard DCSBD.

The schematic drawing of the simplified DCSBD cell is given in Fig. 1. In Fig. 1a the cross-section of the discharge cell is given. The discharge cell is made of a polymeric capsule. In this capsule the system of two electrodes is placed in the gap allowing movement of the powered electrode along one direction. Both electrodes are pressed against the dielectric plate and dipped in insulating transformer-oil bath. The dielectric plate is made of 96% alumina ceramics ($Al_2O_3$) with dimensions of 10 x 10 $cm^2$ and thickness of approximately 0.6 mm.

The electrodes are pressed directly to the surface of the dielectric plate forming two semicircle footprints on the dielectric plate. The rectangular electrode gap is then formed between electrodes. The schematic view of the electrodes' ground plan is given in Fig. 1b. The view plane of the picture is the same as if the paper were the dielectric plate. The rectangular electrode gap between electrodes can be set up with gap-width up to 5 mm and length of electrode edge of 20 mm. The minimum distance between electrodes (electrode gap) is given by the insulating properties of the oil bath. In the presented study the electrode gap was set from 0.55 ± 0.05 mm to 2.0 ± 0.1 mm.

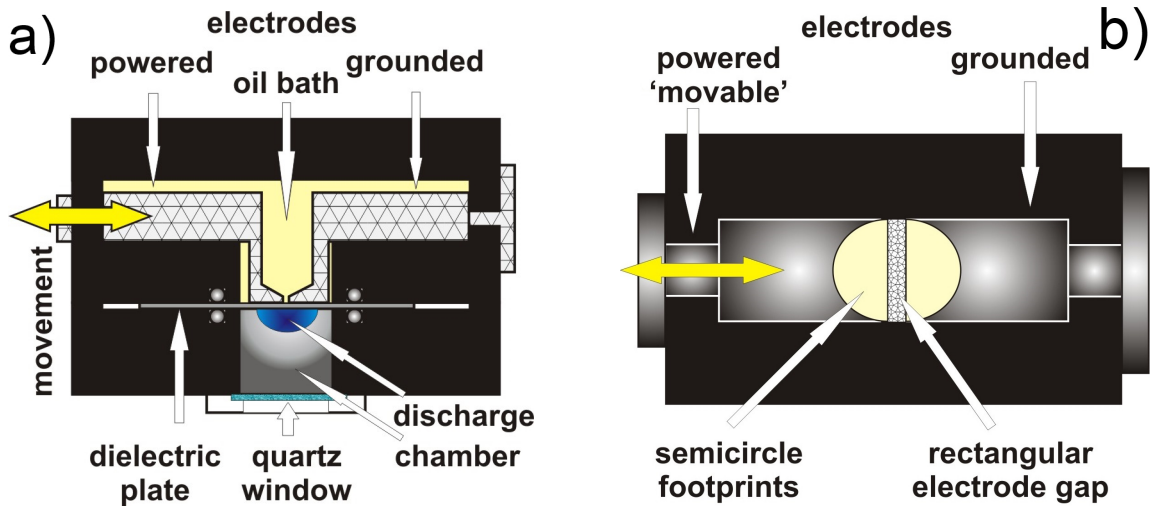


**Figure 1**: Experimental setup – simplified DCSBD discharge cell: a) discharge chamber cross-section b) electrode system ground plan.

The discharge chamber is formed at the opposite side of the dielectric plate than the electrode system (Fig. 1a). The discharge chamber enables the discharge operation in a controlled process gas environment. A quartz window on the opposite side of the discharge chamber enables the optical diagnostics of the discharge.

The experimental setup for DCSBD microdischarges' statistics measurement is given in Fig. 2. The time resolved imaging was set up using the simplified DCSBD discharge cell described in the previous section. The experimental apparatus consists of the simplified DCSBD discharge cell, gas feed supply, electric power supply and diagnostics equipment.

The gas feed supply was made of two Vögtlin Instruments red-y GCR gas flow controllers that were used to set the required process gas atmosphere. A mixture of nitrogen and oxygen gasses of purity better than 99.996% was used. Artificial air with a nitrogen to oxygen ratio of 80:20 was set with total mass flow of 3 slm.

The high-voltage (HV) power supply was used to supply electric power needed for the generation of DCSBD discharge. The HV power supply consists of a LIFETECH HV transformer powered by a high-frequency (HF) low-voltage tuneable generator LIFETECH HF Power Source energized using a stabilized DC power source STATRON 3262. The HV power supply was operated at a sine-wave frequency of approx. 30 kHz and amplitude from 12 to 18 kV. These voltage levels correspond to the level of "just-ignited" discharge and discharge operated at level high above ignition voltage, a.k.a. "overvoltage".

The current-voltage characteristics were recorded using a LeCroy WaveRunner 6100A 1 GHz/5 GSa digital storage oscilloscope coupled with a HV probe Tektronix P6015A 1000:1 (Fig. 2 denoted as Pr1) and Pearson Current Monitor 2877 (Fig. 2 denoted as Pr2). A variable high voltage capacitor was used as the displacement current compensator. The HV capacitor was connected antiparallel through the current probe (Pr2). Tuning the HV capacitor to the capacity close to discharge cell capacity effectively reduces the measured displacement current of the discharge cell which is of the same order as the discharge current for the used discharge cell. This increases the signal-to-noise ratio of discharge current measurements considerably.

The Princeton Instruments PI-MAX 1024RB-25-FG-43 intensified CCD camera (iCCD) equipped with 50 mm, f/2.8 UV lens was used for the synchronized high-speed discharge imaging. The iCCD camera was placed along the axis of symmetry of the discharge cell perpendicular to the DCSBD plasma layer.

To synchronize and semi-automate the measurements, the Agilent 33220A function generator was used as a trigger. The reference signal from the HF generator was used as the synchronization signal for the trigger. The Agilent 33220A fires a series of triggering signals for synchronous capture of iCCD image and current-voltage waveform of the same discharge event.

This setup enables us to take series of synchronized images of the discharge pattern together with its current-voltage characteristics with the resolution of single half-period of high-voltage waveform. In the presented work the series of 100 discharge pattern images of positive, negative and both half-periods were taken with gate times of 17, resp. 34 µs. The iCCD delays were set in a way to guarantee that images represent all discharge events of half-periods that can be identified in current-voltage waveforms.

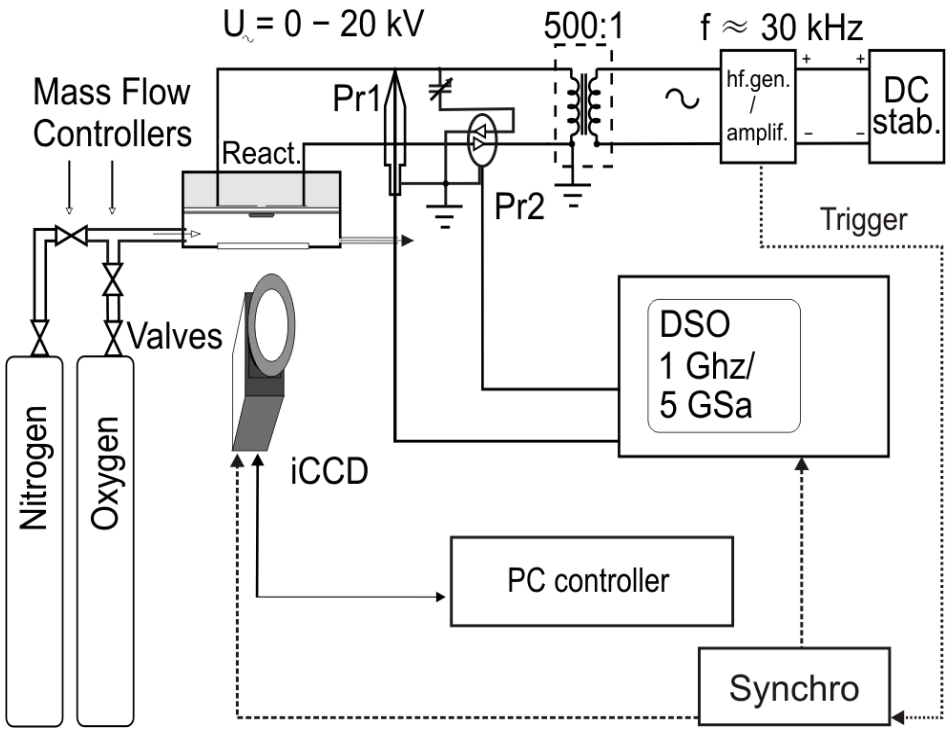


**Figure 2:** Experimental setup: general scheme of discharge setup and time-resolved optical imaging of discharge pattern.

# 3 Results and Discussion

## 3.1 Data acquisition and processing

The DCSBD discharge in steady-state conditions was studied using the experimental setup described above. In order to get the statistical information on DCSBD microdischarges' behaviour 100 discharge events, i.e. half-period or whole period, were recorded for each discharge condition. That gives 300 discharge pattern images and corresponding current-voltage measurements for each studied discharge condition.

In Fig. 3 example iCCD images of discharge patterns are given for DCSBD operated in air. The images of discharge patterns for the input voltage amplitude of 16 kV and electrode gap of 1.5 mm are given as representative examples. The central part of each image corresponds to the electrode gap. Microdischarges cross the gap in the form of bright thin radiant channels called microchannels of 'filaments'. Images represent shots of several microdischarges occurring during one single half/whole period of input high voltage. Fig. 3 a represents positive half-period of discharge. Fig. 3 b represents negative half-period of discharge. Polarity of half-period is taken as a polarity of high voltage put on the left, powered, electrode (Figs 1a and 1b). The electrodes' position and polarity is given for the first image only for better clarity. Fig. 3c represents the whole period of discharge.

In Fig. 4 the typical current-voltage waveforms of DCSBD operated in air are given for the following conditions: HV amplitude of 14 kV, HV frequency of 30 kHz and electrode gap width 0.6 mm. The capacitive current was compensated. The numerous current peaks per half-period of input high-voltage can be seen. The reference triggering signal used for synchronization of time-correlated diagnostics is also given.

Acquired iCCD images and current-voltage waveforms represent a huge amount of raw data to be processed. Therefore the gathered raw data was processed using custom scripts in the MATLAB computational environment to derive the parameters of individual microdischarges.

In the first step of data processing the discharge current corresponding to specified half/whole period of input high-voltage was analyzed. The peak detection algorithm was adopted to evaluate the total number of current peaks, together with their polarity, phase shift and amplitude. An example of current waveform processing is given in Fig. 5. The current pulses corresponding to microdischarge events are marked with crossed circles.

In the second step of data processing the corresponding iCCD images of discharge pattern were processed. The

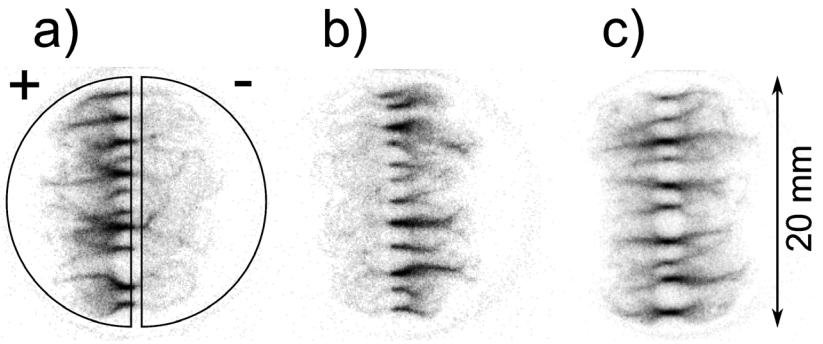


**Figure 3:** Time resolved iCCD images of DCSBD generated in air using sine-wave HV; a) positive half-period of the discharge, b) negative half-period of the discharge and c) whole period of discharge. The position of electrodes and their instantaneous polarities are given for the positive half-period; polarity is switched for the negative half-period.

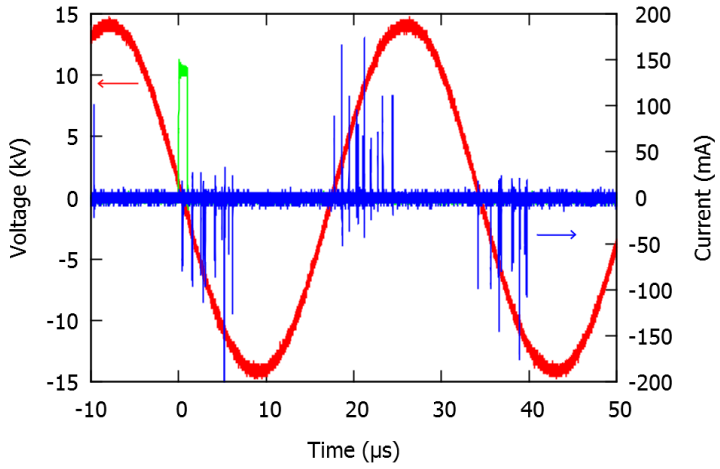


**Figure 4:** Typical current (blue) and voltage (red) waveforms of DCSBD discharge generated using sine-wave HV; position of synchronization signal used for synchronization of iCCD camera and digital storage oscilloscope is also given (green).

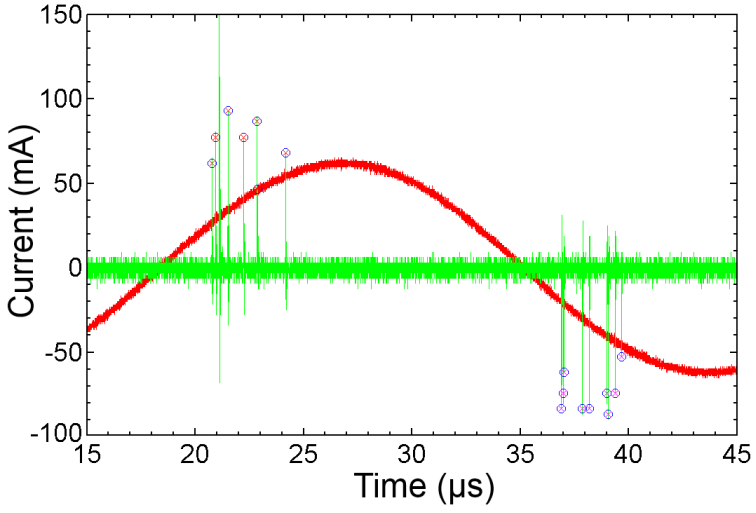


**Figure 5:** Example of discharge current waveform (green) processing: identified microdischarges (marked with crossed circles) are given together with the corresponding voltage waveform (red) to show current/voltage phase shift.

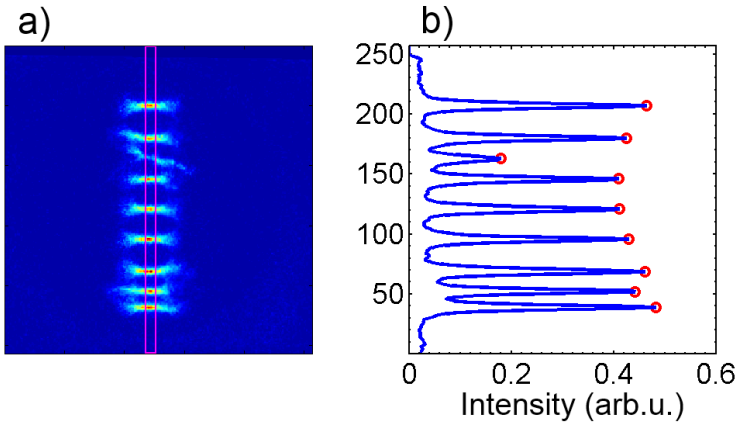


**Figure 6**: Example of iCCD image processing: a) DCSBD discharge pattern in false colours with marked area of interest (electrode gap); b) Corresponding intensity profile with identified filaments marked with circles, on y-axis the row pixel number is given.

narrow rectangular region corresponding to inter-electrode rectangular gap was selected for the analysis of discharge channels of microdischarges (filaments), (Figs. 3 and 6). The total number of individual paths of microdischarges (bright channels) crossing the electrode gap, i.e. filaments, was obtained together with their positions and amplitudes using a similar peak detection algorithm as that used for the discharge current analysis. An example of iCCD image processing is given in Fig. 6. The analysed area of interest is marked in the processed iCCD image, see Fig. 6a. The corresponding intensity profile of the area of interest (above electrode gap) is given in Fig. 6b together with identified individual filaments marked with circles.

From the sets of the individual data for each discharge condition and event, the microdischarges' statistical behavior was derived. The techniques used in the data acquisition and processing cannot identify individual microdischarges in the current waveform if they appear within the fast sequence in the time interval up to 10-20 ns. In that case the recorded current pulse is taken to be a single microdischarge event.

Results of the data processing can be visualized in the forms of distributions of the frequency of appearance of microdischarges, relation matrices of incidence described below or the mean values and deviations of microdischarge parameters.

## 3.2 Statistical parameters of DCSBD microdischarges

The theory of the so-called 'memory effect' [42–44] of DBD says that the time and space appearance of microdischarges is influenced by the remnant electric charges and the excited species in the process gas and on the surface of dielectric barriers. It implies that the reappearance of microdischarges at the close places within the single half-period of the discharge is suppressed by the developed space charge and surface charges which were stored on the dielectric barriers during previous microdischarge event [44]. During the next half-period of the discharge the same mechanism is on the other hand responsible for the local electric field enhancement at the position of some previous microdischarge [43]. This leads to the occurrence of microdischarges at the same positions above the dielectric in following half-periods [45].

It should be mentioned at this point, that the term 'memory effect' is not exclusively used in the description of DBD at atmospheric pressure. The active species behavior was studied thoroughly also in the case of the post discharge phase of low pressure direct-current discharges. This type of 'memory effect' influencing discharge breakdown could be explained in nitrogen afterglow. According to [46] the afterglow is a long time source of atomic nitrogen. The excited (metastable) nitrogen molecules are formed through the process of surface recombination of nitrogen atoms at the discharge tube walls. After collisions of nitrogen metastables with the bare electrode surface the secondary electrons are produced which are able to initiate the next breakdown.

Some important differences between these 'memory effects' should be noted here. The timescales of processes differ considerably in the case of low pressure discharges and atmospheric pressure discharges. In the case of low pressure discharges the lifetime of active species could be of the order of hours [46]. In the case of atmospheric pressure DBDs rather microsecond to millisecond timescales are expected [47,48]. Moreover, in the case

of DBD (DCSBD) there are no bare electrodes, where the effective secondary emission of electrons could take place. Instead the remnant active species influence the places of microdischarge occurrence through the distortion of electric field (in case of charged species at the surfaces) and favoring electron production at the pathways of preceding microdischarges (active species in the volume) [42-45,49,50]. It should be noted also, that the exact processes of 'memory effect' in the case of DBD are not completely understood so far.

The consequences of the described DBD 'memory effect' can be identified in the statistical behavior of DCSBD microdischarges. The set of parameters of microdischarges generated by DCSBD was obtained using data acquisition and the analysis process described in previous section. From these parameters the following parameters were chosen to describe and discuss the influence of discharge conditions on the described 'memory effect' of microdischarges of DCSBD:

- The number of filaments crossing the electrode gap (individual microdischarges' channels) per discharge event;
- Number of microdischarges (individual current peaks) generated per discharge event;
- Current pulses amplitude distribution (as a measure of transferred charge) per discharge event.

The influence of discharge conditions on the statistical distribution of the number of filaments, number of microdischarges and amplitude of current pulses is given in Figs. 7, 8 and 9. The influence of electrode gap width and operating voltage amplitude is shown. Figs. 7, 8 and 9 share the same layout. In subplots marked a) the distribution of the number of individual filaments per discharge event is given. In subplots marked b) the distribution of current pulses' amplitude of individual microdischarges is given. In bottom subplots marked c) the distribution of the number of individual microdischarges per discharge event is given. The distributions given as red bars represent microdischarges from the positive half-period of discharge. The distributions given as green bars represent microdischarges from the whole period of discharge.

From the histograms in Figs. 7, 8 and 9 it is evident that in consecutive half-periods of DCSBD discharge the majority of microdischarges reuse the same paths (microchannels) of microdischarges from the previous half-period. It can be deduced from the comparison of the histograms of the number of filaments and number of current pulses in cases of half-period and whole period (i.e. two consecutive half-periods). The distributions of the number of filaments, i.e. unique microdischarges' paths, remain practically the same for both cases. While the distributions of the number of current pulses shift to nearly double the values of the number of current pulses in the case of the whole period compared to the case of half-period. This behavior is in agreement with the 'memory effect' mechanism. Similar results were published by Akishev [45], where for volume configuration of DBD it was presented that under certain conditions the microdischarges can remain at an exact position for several hundreds of periods.

The histograms of current pulses show also a slight asymmetry towards higher values of number of pulses. In comparison with the position of the distributions maxima the conclusion can be made, that in case of input voltages high above ignition voltage there are more microdischarges (current pulses) than filaments in a single half-period. This means that some of the existing microdischarge paths are reused by some later microdischarges within the same half-period. This behaviour is not predicted by the theory of 'memory effect', so mechanisms other than charge deposition must be responsible for it.

If the electrode gap is then broadened a change in the behavior of microdischarges can be seen. If Figs. 7 and 8 are compared it can be seen that the number of filaments decreases substantially. However, the tendency to reuse some pre-existing discharge path (filament) increases in that case. In that particular case the input voltage was kept the same so the effective electric field in the gas drops. However, the change is even more evident in the case of a wide electrode gap when the input voltage is increased, see Fig. 9. Therefore, there has to be a mechanism other than simply the electric field magnitude that is responsible for the tendency to reuse some pre-existing discharge path (filament) even in the same single half-period of the discharge. Ráheľ et al. posited [51] that the increase of process gas temperature could lower substantially the ignition voltage of DBD. It could be possible that this mechanism is involved in the described behavior of DCSBD microdischarges. Moreover it could be a self-amplifying effect, where the more reused paths could gain a 'temperature advantage' and so under a certain conditions the discharge could fall into the regime of generation of fewer stronger filaments, instead of many weak ones.

A more detailed insight on the correlation of the number of filaments and number of microdischarges per discharge event gives a relation matrix of incidence. Relation matrices can be constructed for microdischarges from half-period as well as whole period of input voltage. Those matrices are given in Figs. 10, 11 and 12, part a) for positive half-period, part b) for whole period of input voltage. Matrices represent evaluation of global behavior

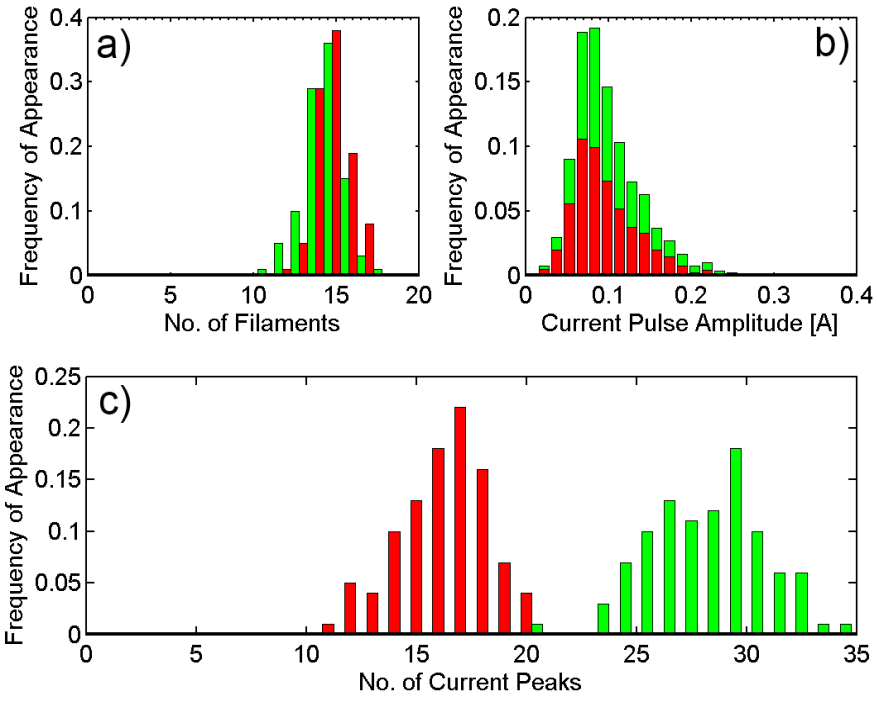


**Figure 7**: Histograms of: a) number of filaments, b) distribution of microdischarges current and c) number of microdischarges. Red bars correspond to positive half-period of discharge; green bars correspond to whole period of the discharge. Discharge conditions were as follows: DCSBD generated using sine-wave HV of the amplitude of 16 kV, electrode gap width set to 0.6 mm.

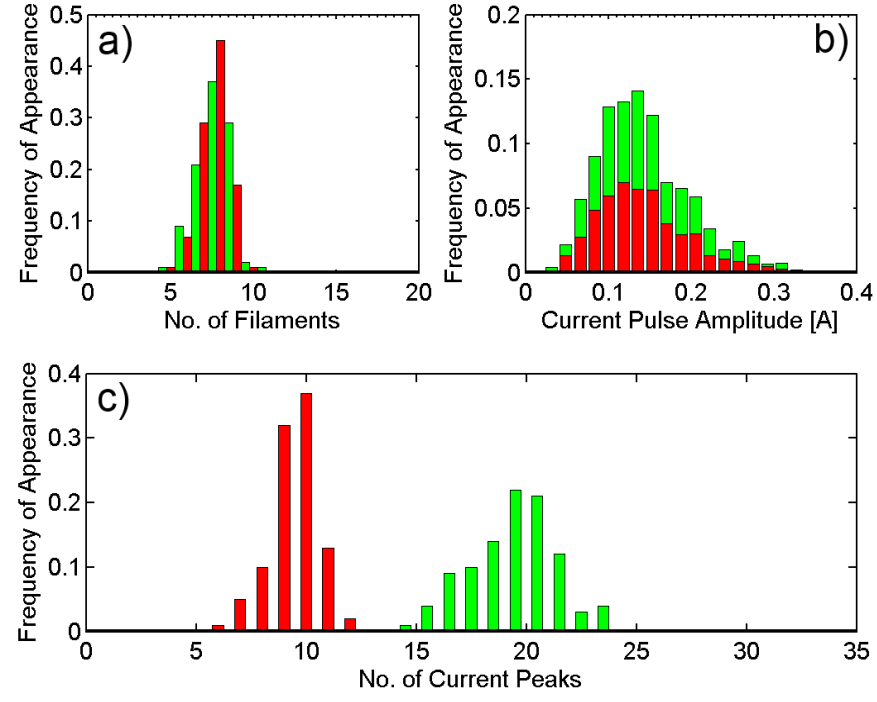


**Figure 8**: Histograms of: a) number of filaments, b) distribution of microdischarges current and c) number of microdischarges. Red bars correspond to positive half-period of discharge; green bars correspond to whole period of the discharge. Discharge conditions were as follows: DCSBD generated using sine-wave HV of the amplitude of 16 kV, electrode gap width set to 2.0 mm.

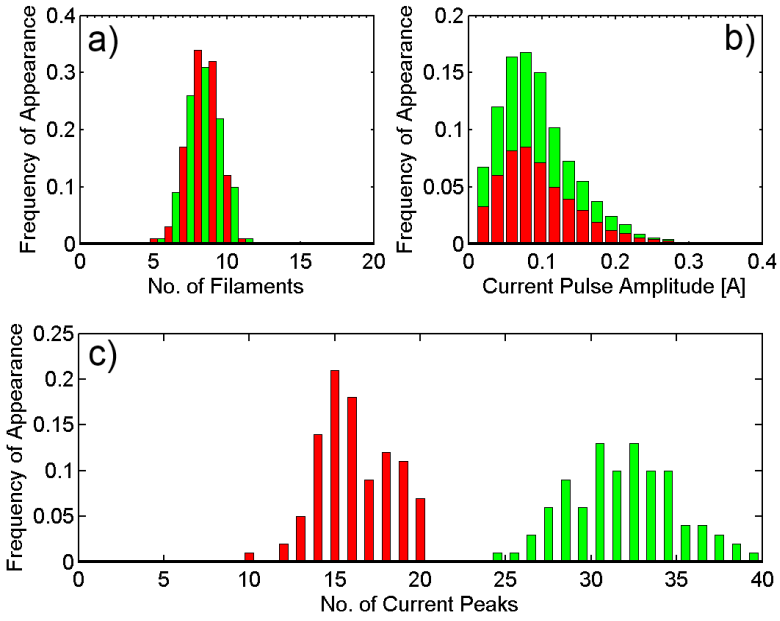


**Figure 9**: Histograms of: a) number of filaments, b) distribution of microdischarges current and c) number of microdischarges. Red bars correspond to positive half-period of discharge; green bars correspond to whole period of the discharge. Discharge conditions were as follows: DCSBD generated using sine-wave HV of the amplitude of 18 kV, electrode gap width set to 2.0 mm.

of microdischarges built from the single microdischarge events. On the x-axis the number of filaments crossing the electrode gap during one half-period (whole period) is given. On the y-axis the corresponding number of current pulses of microdischarges within the same half-period (whole period) is given. The numbers in matrix cells together with the degree of grey of the cells' shading represent numbers of incidence of described events. Cumulative histograms of number of current pulses and number of filaments are given also for better readability.

From the incidence matrices the statistical behaviour of the DCSBD microdischarges can be seen easily. In the case of 1:1 correspondence all events will be positioned along the main diagonal of the incidence matrix. This represents the case where each microdischarge will produce a unique microchannel (filament) crossing the discharge gap. Events above the diagonal in the incidence matrix represent cases where a certain microdischarge path (filament) is used more than once during a single half or whole period. Events below the diagonal in the incidence matrix represent cases where more than one microdischarge path (filament) is generated within the 10–20 ns – the resolution limit of individual current pulse detection. In principle two alternatives could lead to such a case: a) two or more independent current pulses occurred, but not resolved due to the resolution limit; b) two or more microdischarges are generated within a few ns by the mechanism of microdischarge triggering via energetic photons [52–54].

When we compare the behavior of microdischarges of DCSBD operated at narrow electrode gap condition with the behavior at wide electrode gap condition, we can see substantial differences. Please notice the shifted scales (sections) of corresponding incidence matrices in Figs. 10-12. With agreement to the research performed by Hoder [55] on the single-filament DCSBD configuration, the filaments of DCSBD in the regime of 'overvoltage' prefer to extend or branch existing microchannels against formation of new microchannels crossing the electrode gap. The presented data show clear evidence that the substantial number of microdischarges (identified as discharge current peaks or pulses) does not form new microchannels but rather extend or branch existing discharge microchannels.

## 4 Conclusions

In this paper the behavior of microdischarges of diffuse surface coplanar barrier discharge was studied. The microdischarges were studied using correlated time-resolved optical and electrical measurements of DCSBD

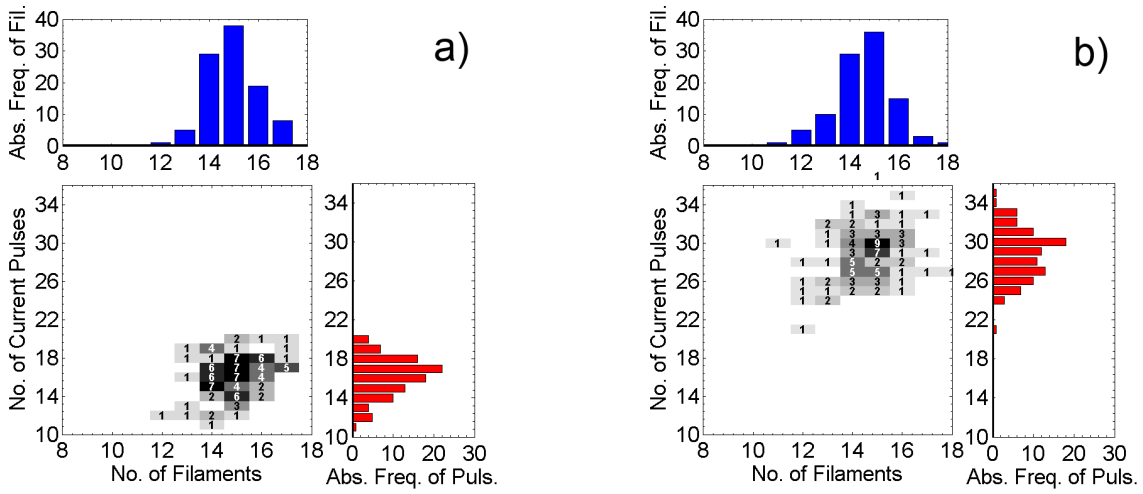


**Figure 10:** Relation matrix of incidence, DCSBD at voltage amplitude 16 kV and electrode gap 0.6 mm; a) positive half-period, b) whole period of discharge.

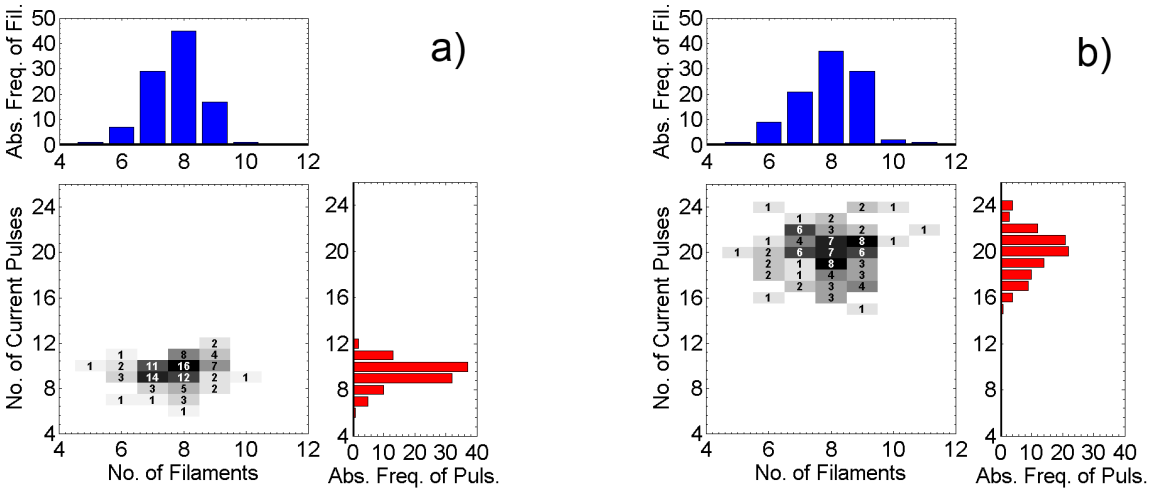


**Figure 11:** Relation matrix of incidence, DCSBD at voltage amplitude 16 kV and electrode gap 2.0 mm; a) positive half-period, b) whole period of discharge.

operated in artificial air. Single-shot pictures of a discharge pattern were taken with the resolution of half-period of input voltage using the presented experimental setup. The collective behavior of DCSBD microdischarges in air was studied using statistical processing of the microdischarges parameters.

Under steady-state conditions the influence of the so-called 'memory effect' was observed. This effect is considered to be responsible for the phenomenon of reusing the pre-existing discharge paths from the previous half-period of the discharge in the following half-period of the discharge. This phenomenon is more pronounced at the wide electrode gap conditions.

The phenomenon of reusing microdischarge paths by following microdischarges can be clearly visualized using the incidence matrices of microdischarges and filaments occurrence in a single half-period or whole-period. It was shown that the microdischarges' paths could be reused by the following microdischarges even in the same half-period of the discharge, in addition to reusing the previous microdischarges' paths during the following half-period of the discharge.

It has been published formerly that under low input voltage conditions the preferred way of microdischarge behavior is a formation of unique microchannel per microdischarge during a single half-period of the discharge

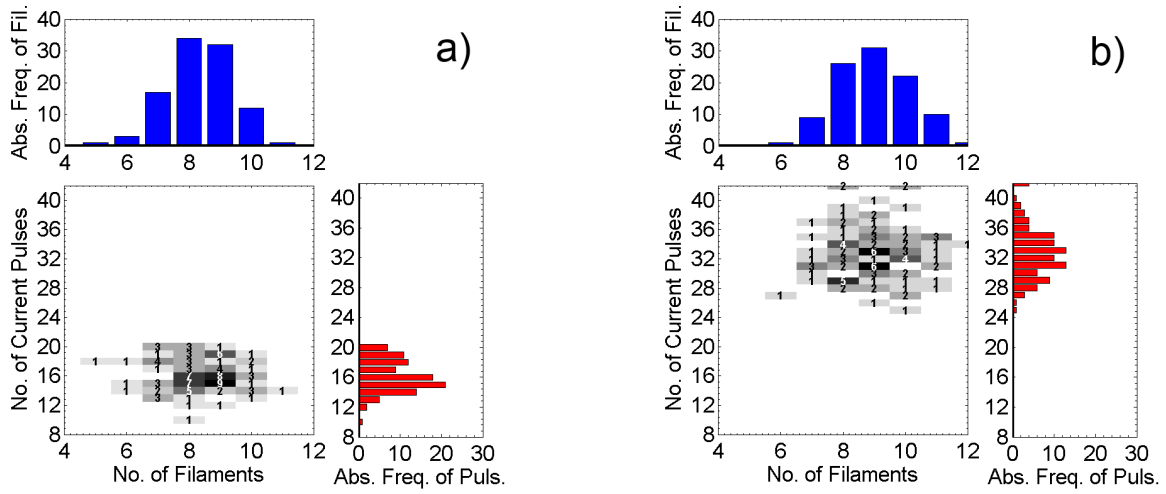


**Figure 12:** Relation matrix of incidence, DCSBD at voltage amplitude 18 kV and electrode gap 2.0 mm; a) positive half-period, b) whole period of discharge.

[28]. On the contrary in the case of substantially increased input voltage ('overvoltage') the preferred behavior of microdischarges during single half-period of the discharge is to reuse pre-existing microchannels (filaments) and/or extend or branch the pre-existing microchannels instead of forming completely new ones.

Results presented in this paper show that the phenomenon of reusing microdischarges' paths is significantly present when the electrode gap is being widened. The obtained results support the previous measurements of DCSBD performed by Hoder in a single-filament DCSBD configuration [55], where two successive microdischarges going along the same path in the same half-period of discharge were studied using cross-correlation spectroscopy at pressure slightly below the atmospheric pressure.

The effect responsible for reusing the discharge paths in the same single half-period of the discharge cannot be satisfactorily explained by the charge deposition. Some other mechanisms must be responsible for that behavior. However, further investigations should be carried out in order to identify them.

**Acknowledgement:** This research has been supported by the project Regional R&D center for low-cost plasma and nanotechnology surface modifications CZ.1.05/2.1.00/03.0086 funded by European Regional Development Fund and project No. GA13-24635S funded by the Czech Science Foundation of the Czech Republic.

## References

[1] Kogelschatz U., Dielectric-barrier Discharges: Their History, Discharge Physics and Industrial Applications, Plasma Chem. Plasma Process., 2003, 23, 1–46

[2] Roth J. R., Industrial Plasma Engineering, Taylor & Francis, Bristol and Philadelphia, 2001

[3] Pappas D., Status and potential of atmospheric plasma processing of materials, J. Vac. Sci. Technol. A Vacuum, Surfaces, Film., 2011, 29, 020801

[4] Temmerman E., Akishev Y., Trushkin N., Leys C., Verschuren J., Surface modification with a remote atmospheric pressure plasma: dc glow discharge and surface streamer regime, J. Phys. D. Appl. Phys., 2005, 38, 505–509

[5] Council regulation (EC) 1907/2006 of 18 december 2006 concerning the Registration, Evaluation, Authorisation and Restriction of Chemicals (REACH), establishing a European Chemicals Agency, amending Directive 1999/45/EC and repealing Council Regulation (EEC) No 793/93 and Commission Regulation (EC) No 1488/94 as well as Council Directive 76/769/EEC and Commission Directives 91/155/EEC, 93/67/EEC, 93/105/EC and 2000/21/EC, OJ L 136/3, 2007

[6] Chirokov A., Gutsol A., Fridman A., Sieber K. D., Grace J. M., Robinson K. S., Analysis of two-dimensional microdischarge distribution in dielectric-barrier discharges, Plasma Sources Sci. Technol., 2004, 13, 623–635

[7] Wagner H.-E., Brandenburg R., Kozlov K. V., Sonnenfeld A., Michel P., Behnke J. F., The barrier discharge: basic properties and applications to surface treatment, Vacuum, 2003, 71, 417–436

[8] Rohani V., Bauville G., Lacour B., Puech V., Duminica F. D., Silberberg E., Study of the treatment's homogeneity in plasma assisted chemical vapour deposition by atmospheric pressure dielectric barrier discharge, Surf. Coatings Technol., 2008, 203, 862–867

[9] Kanazawa S., Kogoma M., Moriwaki T., Okazaki S., Stable glow plasma at atmospheric pressure, J. Phys. D. Appl. Phys., 1988, 21, 838–840
[10] Kong M. G., Electrically efficient production of a diffuse nonthermal atmospheric plasma, IEEE Trans. Plasma Sci., 2003, 31, 7–18
[11] Meiners A., Leck M., Abel B., Efficiency enhancement of a dielectric barrier plasma discharge by dielectric barrier optimization, Rev. Sci. Instrum., 2010, 81, 113507
[12] Foest R., Kindel E., Ohl A., Stieber M., Weltmann K.-D., Non-thermal atmospheric pressure discharges for surface modification, Plasma Phys. Control. Fusion, 2005, 47, B525–B536
[13] Samukawa S., Hori M., Rauf S., Tachibana K., Bruggeman P., Kroesen G., et al., The 2012 Plasma Roadmap, J. Phys. D. Appl. Phys., 2012, 45, 253001
[14] Goossens O., Dekempeneer E., Vangeneugden D., Van de Leest R., Leys C., Application of atmospheric pressure dielectric barrier discharges in deposition, cleaning and activation, Surf. Coatings Technol., 2001, 142–144, 474–481
[15] Bogaerts A., Neyts E., Gijbels R., van der Mullen J., Gas discharge plasmas and their applications, Spectrochim. Acta Part B At. Spectrosc., 2002, 57, 609–658
[16] Borcia G., Anderson C. A., Brown N. M. D., Dielectric barrier discharge for surface treatment: application to selected polymers in film and fibre form, Plasma Sources Sci. Technol., 2003, 12, 335–344
[17] Pietsch G. J., Gibalov V. I., Dielectric barrier discharges and ozone synthesis, Pure Appl. Chem., 1998, 70, 1169–1174
[18] Kogelschatz U., Eliasson B., Egli W., Dielectric-Barrier Discharges. Principle and Applications, Le J. Phys. IV, 1997, 07, C4-47–C4-66
[19] Šimor M., Ráhel' J., Vojtek P., Černák M., Brablec A., Atmospheric-pressure diffuse coplanar surface discharge for surface treatments, Appl. Phys. Lett., 2002, 81, 2716
[20] Černák M., Ráhel' J., Kováčik D., Šimor M., Brablec A., Slavíček P., Generation of Thin Surface Plasma Layers for Atmospheric-Pressure Surface Treatments, Contrib. to Plasma Phys., 2004, 44, 492–495
[21] Černák M., Kováčik D., Ráhel' J., St'ahel P., Zahoranová A., Kubincová J., et al., Generation of a high-density highly non-equilibrium air plasma for high-speed large-area flat surface processing, Plasma Phys. Control. Fusion, 2011, 53, 12, 124031
[22] Eliasson B., Hirth M., Kogelschatz U., Ozone synthesis from oxygen in dielectric barrier discharges, J. Phys. D. Appl. Phys., 1987, 20, 1421–1437
[23] Gibalov V. I., Pietsch G. J., The development of dielectric barrier discharges in gas gaps and on surfaces, J. Phys. D. Appl. Phys., 2000, 33, 2618–2636
[24] Kogelschatz U., Collective phenomena in volume and surface barrier discharges, J. Phys. Conf. Ser., 2010, 257, 012015
[25] Bruggeman P., Brandenburg R., Atmospheric pressure discharge filaments and microplasmas: physics, chemistry and diagnostics, J. Phys. D. Appl. Phys., 2013, 46, 464001
[26] Hoder T., Šíra M., Kozlov K. V., Wagner H.-E., Investigation of the coplanar barrier discharge in synthetic air at atmospheric pressure by cross-correlation spectroscopy, J. Phys. D. Appl. Phys., 2008, 41, 035212
[27] Hoder T., Šíra M., Kozlov K. V., Wagner H.-E., 3D Imaging of the Single Microdischarge Development in Coplanar Barrier Discharges in Synthetic Air at Atmospheric Pressure, Contrib. to Plasma Phys., 2009, 49, 381–387
[28] Cech J., Hanusova J., Stahel P., Slavicek P., Diffuse Coplanar Surface Barrier Discharge In Nitrogen: Microdischarges Statistical Behavior, Acta Polytech., 2013, 53, 127–130
[29] Čech J., Sťahel P., Navrátil Z., The influence of electrode gap width on plasma properties of diffuse coplanar surface barrier discharge in nitrogen, Eur. Phys. J. D, 2009, 54, 259–264
[30] Čech J., St'ahel P., Navrátil Z., Černák M., Space and Time Resolved Optical Emission Spectroscopy of Diffuse Surface Coplanar Barrier Discharge in Nitrogen, Chem. List., 2008, 102, 1348–1351
[31] Skácelová D., Danilov V., Schäfer J., Quade A., Sťahel P., Černák M., et al., Room temperature plasma oxidation in DCSBD: A new method for preparation of silicon dioxide films at atmospheric pressure, Mater. Sci. Eng. B, 2013, 178, 651–655.
[32] Prysiazhnyi V., Vasina P., Panyala N. R., Havel J., Cernak M., Air DCSBD plasma treatment of Al surface at atmospheric pressure, Surf. Coatings Technol., 2012, 206, 3011–3016
[33] Homola T., Matoušek J., Medvecká V., Zahoranová A., Kormunda M., Kováčik D., et al., Atmospheric pressure diffuse plasma in ambient air for ITO surface cleaning, Appl. Surf. Sci., 2012, 258, 7135–7139
[34] Homola T., Matoušek J., Hergelová B., Kormunda M., Wu L. Y. L., Černák M., Activation of poly(ethylene terephthalate) surfaces by atmospheric pressure plasma, Polym. Degrad. Stab., 2012, 97, 2249–2254
[35] Černáková L., Szabová R., Wolfová M., Buček A., Černák M., Surface modification of polypropylene nonwoven after plasma activation at atmospheric pressure, Fibres Text. East. Eur., 2007, 15, 121–123
[36] Massines F., Gherardi N., Naudé N., Ségur P., Recent advances in the understanding of homogeneous dielectric barrier discharges, Eur. Phys. J. Appl. Phys., 2009, 47, 22805
[37] Fanelli F., d'Agostino R., Fracassi F., Effect of Gas Impurities on the Operation of Dielectric Barrier Discharges Fed with He, Ar, and Ar-C3F6, Plasma Process. Polym., 2011, 8, 557–567
[38] Brandenburg R., Navrátil Z., Jánský J., St'ahel P., Trunec D., Wagner H.-E., The transition between different modes of barrier discharges at atmospheric pressure, J. Phys. D. Appl. Phys., 2009, 42, 085208
[39] Fang Z., Qiu Y., Zhang C., Kuffel E., Factors influencing the existence of the homogeneous dielectric barrier discharge in air at atmospheric pressure, J. Phys. D. Appl. Phys., 2007, 40, 1401–1407
[40] Černák M., Černáková L., Hudec I., Kováčik D., Zahoranová A., Diffuse Coplanar Surface Barrier Discharge and its applications for in-line processing of low-added-value materials, Eur. Phys. J. Appl. Phys., 2009, 47, 22806
[41] Štefečka M., Kando M., Černák M., Korzec D., Finantu-Dinu E. G., Dinu G. L., et al., Spatial distribution of surface treatment efficiency in coplanar barrier discharge operated with oxygen–nitrogen gas mixtures, Surf. Coatings Technol., 2003, 174–175, 553–558
[42] Akishev Y., Aponin G., Balakirev A., Grushin M., Karalnik V., Petryakov A., et al., 'Memory' and sustention of microdischarges in a steady-state DBD: volume plasma or surface charge?, Plasma Sources Sci. Technol., 2011, 20, 024005
[43] Bogaczyk M., Nemschokmichal S., Wild R., Stollenwerk L., Brandenburg R., Meichsner J., et al., Development of Barrier

Discharges: Operation Modes and Structure Formation, Contrib. to Plasma Phys., 2012, 52, 847–855

[44] Chirokov A., Gutsol A., Fridman A., Atmospheric pressure plasma of dielectric barrier discharges, Pure Appl. Chem., 2005, 77, 487–495

[45] Akishev Y., Aponin G., Balakirev A., Grushin M., Karalnik V., Petryakov A., et al., Spatial-temporal behavior of individual microdischarges in dielectric barrier discharge, Acta Tech. ČSAV (Československá Akad. Věd), 2011, 56, T3–T14

[46] Marković V. L., Petrović Z. L., Pejović M. M., Surface recombination of atoms in a nitrogen afterglow, J. Chem. Phys., 1994, 100, 8514-8521

[47] Kettlitz M., Höft H., Hoder T., Reuter S., Weltmann K.-D., Brandenburg R., On the spatio-temporal development of pulsed barrier discharges: influence of duty cycle variation, J. Phys. D. Appl. Phys., 2012, 45, 245201

[48] Šimek M., Ambrico P. F., De Benedictis S., Dilecce G., Prukner V., Schmidt J., N2(A3 ∑+u) behaviour in a N2 –NO surface dielectric barrier discharge in the modulated ac regime at atmospheric pressure, J. Phys. D. Appl. Phys., 2010, 43, 124003

[49] Bogaczyk M., Nemschokmichal S., Wild R., Stollenwerk L., Brandenburg R., Meichsner J., et al., Development of Barrier Discharges: Operation Modes and Structure Formation, Contrib. to Plasma Phys., 2012, 52, 847–855

[50] Manley T. C., Electric characteristics of the ozonator discharge, Trans. Electrochem. Soc., 1943, 84, 83-96

[51] Ráhel' J., Szalay Z., Morávek T., DBD breakdown voltage at elevated temperatures, Book of abstracts, 5th Central European Symposium on Plasma Chemistry (25-29 August 2013, Balatonalmádi, Hungary), RCNS HAS Budapest, Hungary, 2013, 115–116

[52] Allegraud K., Guaitella O., Rousseau A., Spatio-temporal breakdown in surface DBDs: evidence of collective effect, J. Phys. D. Appl. Phys., 2007, 40, 7698–7706

[53] Dong L., Yin Z., Li X., Chai Z., Wang L., Spatiotemporal dynamics of discharge filaments in dielectric barrier discharges, J. Electrostat., 2003, 57, 243–250

[54] Kashiwagi Y., Itoh H., Synchronization of positive surface streamers triggered by vacuum ultraviolet in atmosphere, J. Phys. D. Appl. Phys., 2006, 39, 113–118

[55] Hoder, T., Studium filamentu koplanárního bariérového výboje, PhD thesis, Masaryk University, Brno, Czech Republic, 2009, (in Czech)